Journal Name

ARTICLE

Controlling the melting transition of semi-crystalline self-assembled block copolymer aggregates: Controlling release rates of Ibuprofen

Received 00th January 20xx,
Accepted 00th January 20xx

DOI: 10.1039/x0xx00000x

www.rsc.org/

O.R. Monaghan,[a] P.H.H. Bomans,[b] N.A.J.M. Sommerdijk,*[b] and S.J. Holder*[a]

Bicontinuous nanospheres and multi-lamellar micelles were self-assembled from poly[ethylene oxide]-*block*-(poly[octadecyl methacrylate]-*random*-poly[docosyl methacrylate]), (PEO-*b*-[PODMA-*co*-PDSMA]) where PEO is the hydrophilic block (25 wt%) and PODMA/PDSMA is the semi-crystalline hydrophobic block (75 wt%) that gives a thermoresponsive component to the self-assembled aggregates. By varying the relative molar proportion of DSMA to ODMA (from 0:1 to 1:0) in the synthesis of the copolymers by atom transfer radical polymerisation, the melting transition ™ of the hydrophobic block could be varied from 21.5 to 41.1°C in the solid state. When self-assembled in aqueous dispersions the T_m range was 23.4 to 41.3°C, closely matching that of the solid samples. Preliminary analysis of the rate of release of ibuprofen from three of the block copolymer aggregates demonstrated that the rate of release was correlated with the degree of crystallinity of the hydrophobic block and that increasing temperature causes melting and a significantly enhanced release rate.

Introduction

Amphiphilic block copolymers, that have an affinity for two different types of environment, self-assemble in aqueous media to form a variety of aggregate structures, most commonly micelles and vesicles.[1] The use of these aggregates as nanocarriers for controlled drug delivery has been widely studied and considerable research has been devoted to the use of thermo-responsive aggregates; i.e. micelles or vesicles that release, or accelerate the rate of release of, encapsulated compounds upon a change in temperature. Most of these systems have been based upon a thermoresponsive hydrophilic component of a block copolymer with well-defined lower critical transition temperatures, probably the most utilised being poly(N-isopropylacrylamide).[1-3] The use of the hydrophobic component of block copolymers as the thermo-responsive component has been considerably less studied.[4, 5] We have previously reported on the thermo-responsive nature of bicontinuous polymer nanospheres (BPNs) that self-assembled in aqueous dispersions from PEO-*b*-PODMA.[6] BPNs are discrete aggregates that have a twisted hydrophobic network interconnected with that of a hydrophobic moiety. The self-assembly of BPNs from PEO-*b*-PODMA has been investigated previously by Holder and Sommerdijk *et al.* and it was found that the weight fraction of the hydrophilic block (PEO) should be between 15-25% with the molecular weight at < 17 kDa for BPNs to form.[7] In this case the hydrophobic PODMA block exhibited a melting transition due to the crystallisation of the long alkyl side chains. It was subsequently established that the T_m of the ODMA block affected the rate of release of a hydrophobic compound into the surrounding aqueous medium; pyrene was encapsulated within the BPNs and above the T_m of the PODMA block (21°C), the rate of release increased significantly.[8]

A potential advantage of bicontinuous nanospheres over 'classical' spherical core-corona spherical micelles is their size and high hydrophobic polymer content. Bicontinuous nanospheres are predominantly found in the size range 100 to 500 nm in diameter, an order of magnitude larger than micelles formed from equivalent sized block copolymers (typically 2 to 10 nm). Furthermore their size can be controlled through variation in preparation conditions.[9] This means that such aggregates are potentially useable in therapies that rely upon the enhanced permeability and retention (EPR) effect in tumour treatment.[10, 11] One of the factors influencing EPR in tumour tissue is the particle size, with diameters between 100 and 200 nm often quoted as the optimum to enhance retention and reduce removal by the liver and reticuloendothelial system.[12] The higher hydrophobic component of the core in the larger diameter aggregates also offers the means to transport significantly higher

[a] *Functional Materials Group, School of Physical Sciences, University of Kent, Canterbury, Kent CT2 7NH, UK. E-mail: S.J.Holder@kent.ac.uk*
[b] *1) Laboratory of Materials and Interface Chemistry & Center for Multiscale Electron Microscopy, Eindhoven University of Technology, P.O. Box 513, d. 5600 MB Eindhoven, The Netherlands. E-mail: N.Sommerdijk@tue.nl*
2) Institute for Complex Molecular Systems, Eindhoven University of Technology, PO Box 513, 5600 MB Eindhoven, The Netherlands
† *Electronic Supplementary Information (ESI) available: ^1H and ^{13}C NMR of all block copoylmers, GPC traces of PEO macroinitiator and block copolymers, DLS plots and data table, TEM and cryo-TEM images .*

concentrations of hydrophobic molecules through aqueous media than spherical micelles.

The ability of poly acrylate and poly methacrylate side chains to crystallise has been well documented and investigated. Rehberg and Fisher studied the brittle points of polyacrylates and poly(methacrylates) and found that upon an increase in carbons within the alkyl side chain the brittle points decrease up to 8 carbons for acrylates and 12 carbons for methacrylates, above which the brittle points increased.[13] This was attributed to the increase in the melting point of the side chains[14, 15] Jordan *et al.* investigated the crystallinity of the alkyl side chains in poly(*n*-alkyl acrylates) and they established that only the outer methylene units contributed to the crystal lattice.[16, 17] This was also independently confirmed by several other investigators, it was proposed that the 8-9 methylene units closest to the polymer backbone do not contribute to the side chain crystallinity.[15, 18, 19] Thus for both semi-crystalline poly(alkyl acrylate)s and poly(alkyl methacrylate)s the longer the side–chain the higher the T_m of the poly(alkyl(meth)acrylate).[15, 16] Furthermore it has been demonstrated that by copolymerising (meth)acrylate monomers the T_m of the resultant statistical copolymers can be manipulated to occur within a given range typically between the T_m values of the two homopolymers, with the exact value dependent upon the ratio of monomers within the structure.[20-23] By copolymerising ODMA with an alkyl methacrylate monomer with a higher melting transition temperature it should therefore be possible to manipulate the melting transition of the alkyl methacrylate block of a PEO-*b*-poly(alkyl methacrylate) copolymer and thereby the melting transition of the aggregates formed. In this paper we will describe the successful synthesis of a range of poly(ethylene oxide)-*block*-poly(alkyl methacrylate) homopolymers and copolymers that display T_m values between 21 and 42°C with varying degrees of crystallinity. These copolymers furthermore self-assemble to form bicontinuous and lamellar aggregates in aqueous solution that retain crystallinity and which show a T_m range between 23 and 42°C. We will also report on our preliminary studies on the controlled release of ibuprofen from some of these aggregates. Ibuprofen is a non-steroidal anti-inflammatory drug (NSAID) and there is considerable interest in the application of NSAIDs in cancer treatment with recent evidence suggesting such compounds reduce relapses and mortality rates.[24-26]

Experimental

Materials and Apparatus

Triethylamine (TEA) (99 %), 2-bromoisobutryl bromide (BIBB) (98 %), 4-dimethylamino pyridine (DMAP) (99 %), poly (ethylene glycol) methyl ether (M_n ca. 2000 and 5000 g/mol) (PEGME), octadecyl methacrylate (ODMA), copper (I) bromide (98%), N,N,N',N'',N''-pentamethyldiethylenetriamine (PMDETA) (99%) were all used as received from Sigma-Aldrich. Aluminium oxide (activated, neutral, for column chromatography 50-200µm) and sodium bicarbonate (analytical reagent grade) were purchased from Acros Organics. Tetrahydrofuran (analytical reagent grade), isopropyl alcohol, ethanol (analytical grade), triethylamine, acetonitrile (HPLC grade) and orthophosphoric acid were purchased from Fisher Scientific. 4-Isobutyl-alpha-methylphenylacetic acid, 99 % (Ibuprofen) was purchased from Alfa Aesar. Xylene was purchased from BDH Lab Supplies. The deuterated solvent used in ^{1}H-NMR was used as purchased from Cambridge Isotope Laboratories Incorporated. Hydrochloric acid (36%) was purchased from Fisher Scientific and diluted with distilled water to make a 10% concentration. Dichloromethane (analytical reagent grade) was purchased from Fisher Scientific and dried and distilled over calcium hydride before use.

All reactions were performed under inert atmosphere using schlenk techniques. The infra-red spectra were recorded using a Shimadzu FT-IR spectrometer. ^{1}H-NMR and ^{13}C-NMR spectra were obtained by dissolving the sample in deuterated chloroform ($CDCl_3$) and recorded on a JEOL ECS-400 spectrometer (400 MHz) at 25°C. Molecular weight averages and dispersity indices were calculated using size exclusion chromatography on a Polymer Laboratories PL-GPC 50 plus gel permeation chromatography system (GPC) using two 5 µm mixed C PLgel columns at 40°C. The GPC was calibrated using poly(methyl methacrylate) standards (PMMA). The samples were all dissolved in THF and detected by a refractive index detector.

Self-assembly Procedures

The BCPs were used as synthesised. Distilled water was used as obtained. *A* syringe pump (220 Voltz, 0.1 Amps, 50Hz) was used from Semat technical Limited at 0.085 mL per minute. A 5 mL dialysis cassette was used with dialysis membrane (MWCO-12-14000 Daltons) from MEDICELL international Ltd.

Block copolymer aggregates. The BCP (0.5 g) was dissolved in THF (6 mL) and stirred at 45°C (oil bath). Deionised water was then added drop-wise (at 5.15 mL/hr) to the stirred solution via a syringe pump to make the total volume up to 10 mL. After the addition of the water the solution was either transferred to a dialysis chamber and sealed with a dialysis membrane or sealed in dialysis tubing with clips, then left spinning in 3L of deionised water pre-heated to 45°C for 24 hours. Over the 24 hours the water was changed twice. The aggregates formed then analysed using dynamic light scattering (DLS) and transmission electron microscopy (TEM) to determine the size and polydispersity of the aggregates.

Bock copolymer–ibuprofen aggregates. The BCP (0.1 g) and Ibuprofen (0.02 g) were dissolved in 6 mL of THF and left stirring at 10°C. Deionised water (4 mL) was then added drop-wise to the stirred solution via a syringe pump to make the total volume up to 10 mL. After the addition of the water the solution was sealed in dialysis tubing with clips and then dialysed against distilled water at 10°C for 3 days. Over the 3 days the water was changed twice. The aggregates formed were then analysed using dynamic light scattering (DLS) and

transmission electron microscopy (TEM) to determine the size and polydispersity of the aggregates.

Dynamic Light Scattering

Dynamic Light Scattering (DLS) measurements were obtained on a Malvern High Performance Particle Sizer (Nano Zetasizer HPPS HPP5001) with a laser at a wavelength of 633 nm. The measurements were taken using a clean quartz cuvette containing a 1 mL sample. Measurements were taken at 25°C for the BCP aggregates, and 10°C for the ibuprofen containing aggregates. The temperature was set and the sample was left to equilibrate at this temperature for 10 minutes, after this 10 measurements were taken and an average was obtained.

Transmission Electron Microscopy

Transmission electron microscopy (TEM) was carried out on all the self-assembled samples using a JEOL JEM (200-FX) TEM (120kV). 5 µl of the sample was pipetted onto a carbon-coated copper grid (200 mesh) and left for 5 minutes and then removed using suction. Using 5 µl of 5 % uranyl acetate the grid was then stained, and excess fluid removed via suction.

Cryo-Transmission Electron Microscopy

Cryo-Transmission electron microscopy (cryo-TEM) was performed on a FEI Cryo-Titan with a field emission gun operating at 300 kV. The sample vitrification process was as follows; 3 µl of the self-assembled solution was pipetted onto a surface plasma treated (Cresington Carbon Coater 208) Quantifoil holey (Cu 200 mesh) grid inside a FEI Vitrobot chamber (set to 100% humidity at room temperature to prevent sample evaporation). The sample was then blotted and plunged into liquid ethane cooled by liquid nitrogen.

Differential Scanning Calorimetry

Differential scanning calorimetric (DSC) analysis was carried out on the bulk samples along with the 5 wt% aggregate solutions using a Netzsch DSC 200 Phox with a heating range of -150-600°C. Thermal analyses were carried out across the range -20°C to 80°C for bulk and 5 to 80°C for the 5 wt% aggregate solutions. The samples were heated at a rate of 10°C/min. The samples were heated and cooled two times with the first heating run not taken into account to allow for any artifacts present. The transition values were therefore taken from the second heating run. The bulk samples were measured against an empty aluminium pan as the reference and an aluminium pan filled with an equivalent weight of water was used as the reference for the 5 wt% solutions.

High performance Liquid Chromatography

HPLC was carried out on a Dionex UltiMate 3000 UHPLC with a UV detector set to 222 nm. A modified literature method was used as follows;[26] A Nucleosil C18 5 micron column was used (150 mm x 4.6 mm) as the stationary phase with an isocratic mobile phase of triethylamine and orthophosphoric acid buffer (1:1.5) and acetonitrile in the ratio of 40:60 buffer:acetonitrile. The method was carried out at with a flow rate of 1 mL/min and the column temperature kept at 25°C. The total run time for each chromatogram was 10 minutes with a blank in between each run.

Construction of Ibuprofen Calibration Curve

Ibuprofen was dissolved in distilled water (1 L) and left stirring for 24 hours to ensure complete dissolution. A serial dilution was carried out on this solution (25 mL) by 50 % each time until a series of 10 solutions were obtained with a concentration range of 1.00 X 10^{-5} mol dm^{-3} to 1.96 x 10^{-7} mol dm^{-3}. The solutions were then analysed using HPLC, following the method above, to construct a calibration curve (ESI).

Controlled release of Ibuprofen

The self-assembled BCP and ibuprofen solution (1 mL) was transferred to a 1 mL QuixSep dialyser and dialysed against 750 mL of distilled water for 6 hours with 5 mL of the dialysing water collected at time intervals throughout the 6 hour period. These 5 mL aliquots were then analysed using HPLC to determine the ibuprofen concentration with use of the calibration curve.

Synthesis of poly (ethylene oxide) macroinitiators via esterification (I1-I5)

A literature method was followed as the typical procedure for the synthesis of all PEO macrointiators;8 2-bromoisobutryl bromide (11.50 g, 50 mmol), triethylamine (5.06 g, 50 mmol) and 4-dimethylamino pyridine (6.11 g, 50 mmol) dissolved in anhydrous dichloromethane were added to a round bottom flask and stirred, the flask was then sealed. PEGME (Mn 2000) (50 g, 25 mmol) dissolved in 100 mL of anhydrous dichloromethane was added drop wise to the mixture at 0°C for 1 hour under nitrogen. The mixture was then stirred for a further 18 hours at room temperature. The mixture was filtered to remove the amine salt and half the solvent was evaporated off (rotary evaporator). The mixture was made up to 100 mL with dichloromethane. In a separating funnel the mixture was then washed twice with a saturated sodium bicarbonate solution and then twice with hydrochloric acid (10 %). The organic layer (bottom) was then collected and dried using anhydrous magnesium sulphate for 1 hour. The solution was filtered, the solvent evaporated off (rotary evaporator) and the product was dried in a vacuum oven overnight to produce a white waxy solid. The compound was characterised using ^{1}H-NMR, FT-IR and GPC.

(I1) ^{1}H NMR (400 MHz, $CDCl_3$, ppm) δ: 1.94 (singlet, 6H, $(C\mathbf{H_3})_2C$-), 3.38 (singlet, 3H, -O**C**$\mathbf{H_3}$), 3.65 (broad peak, 4H, -O$\mathbf{CH_2}C\mathbf{H_2}$-), 3.82 (triplet, 2H, -$\mathbf{CH_2}$O-), 4.33 (triplet, 2H, COO$\mathbf{CH_2}$-). **(I1) ^{13}C NMR ($CDCl_3$, ppm) δ:** 31.3 (Br-C($\mathbf{C}H_3)_2$-), 56.2 (Br-**C**-), 59.5 (**C**H_3-O-), 65.6 (-COO-**C**H_2-CH_2-), 69.2 (-COO-CH_2-**C**H_2-),71.0 (-O-**C**H_2**C**H_2-), 72.4 (CH_3O-**C**H_2-), 172.1 (Br-C(CH_3)$_2$-**C**OO-). **(I1) FTIR (cm^{-1}):** 2883 C-H stretch, 1734 C=O stretch, 1465 C-H bend, 1099 C-O stretch, 528 C-Br stretch. I2 gave identical signals.

Synthesis of poly(ethylene oxide)-*block*-(poly(octadecyl methacrylate)

A literature method was modified and used as the typical procedure for the synthesis of PEO-*b*-PODMA block copolymer;[6] Cu (I) Br (30 mg, 0.21 mmoles) was placed in a 25 mL Schlenk tube with a magnetic stirrer. The PEO macroinitiator (1.00 g, 0.42 mmoles) was dissolved in xylene:IPA mixture (9:1) (4 mL) and then added to the Schlenk tube along with PMDETA (73 mg, 0.42 mmoles) and ODMA (2.78 g, 8.2 mmoles). The Schlenk tube was sealed and the mixture was degassed (N_2) for 1 hour. The mixture was then stirred at 95°C for 24 hours under nitrogen. After 24 hours the reaction was stopped by exposure to air and diluting with THF. The mixture was run through an alumina column to remove the catalyst and ligand and half the solvent was evaporated off (rotary evaporator). The polymer was precipitated out into ethanol drop wise at 0°C. The block copolymer was characterised using ^{1}H-NMR, ^{13}C-NMR, FT-IR and GPC.

^{1}H NMR (400 MHz, $CDCl_3$, ppm) δ: 0.88 (triplet, 3H, -$(CH_2)_{17}$-C**H_3**), 1.02 (broad peak, 3H, -CH_2-C-C**H_3**), 1.28 (broad peak, 30H, -(C**H_2**)$_{15}$-), 1.60 (broad peak, 2H, -C**H_2**-$(CH_2)_{15}$-), 3.38 (singlet, 3H, C**H_3**O-), 3.64 (triplet, 4H, -O-C**H_2CH_2**-O), 3.91 (broad peak, 2H, -COO-C**H_2**-). **^{13}C NMR ($CDCl_3$, ppm) δ:** 14.23 (-CH_2CH_2**C**H_3), 22.8 (-CH_2**C**H_2CH_3), 32.04 (-**C**$H_2CH_2CH_3$), 29.5 (-$CH_2(CH_2)_{10}$**C**H_2-), 29.8 (-CH_2(**C**H_2)$_{10}CH_2$-), 26.2 (-COO-CH_2CH_2**C**H_2-), 28.20 (-COO-CH_2**C**H_2CH_2-), 65.1(-COO-**C**$H_2CH_2CH_2$-), 70.65 (-O-**C**H_2**C**H_2O-). **FTIR (cm^{-1}):** 2916 C-H stretch, 2848 C-H stretch, 1728 C=O stretch, 1465 C-H stretch, 1242 C-C stretch, 1145 C-O stretch, 721 C-H rock.

Synthesis of poly(ethylene oxide)-*block*-Poly(docosyl methacrylate)

The method for the synthesis of PEO-*b*-PDSMA was as follows; Cu(I)Br (33 mg, 0.2315 mmoles) was placed in a 25 ml Schlenk tube with a magnetic stirrer. The PEO Macroinitiator (1.00 g, 0.46 mmoles) was dissolved in a xylene:IPA mixture (9:1) (4 mL) and then added to the Schlenk tube along with PMDETA (80 mg, 0.46 mmoles) and docosyl methacrylate (DSMA) (2.19 g, 5.55 mmoles). The Schlenk tube was sealed and the mixture was degassed (N_2) for 1 hour. The mixture was then stirred at 95°C for 24 hours under nitrogen. After 24 hours the reaction was stopped by exposure to air and diluting with THF. The mixture was run through an alumina column to remove the catalyst and ligand and half the solvent was evaporated off (rotary evaporator). The polymer was precipitated out into ethanol drop wise at 0°C. The block copolymer was characterised using ^{1}H-NMR, ^{13}C-NMR, FT-IR and GPC.

(P6) ^{1}H NMR (400 MHz, $CDCl_3$, ppm) δ: 0.88 (triplet, 3H, -$(CH_2)_{21}$-C**H_3**), 1.02 (broad peak, 3H, -CH_2-C-C**H_3**), 1.28 (broad peak, 38H, -(C**H_2**)$_{19}$-), 1.60 (broad peak, 2H, -C**H_2**-$(CH_2)_{19}$-), 3.38 (singlet, 3H, C**H_3**O-), 3.65 (broad triplet, 4H, -O-C**H_2CH_2**-O-), 3.92 (broad peak, 2H, -COO-C**H_2**). **(P6) ^{13}C NMR ($CDCl_3$, ppm) δ:** 14.2 (-CH_2CH_2**C**H_3), 18.5 (-C(**C**H_3)$_2$-) 22.7 (-CH_2**C**H_2CH_3), 26.2 (-COO-CH_2CH_2**C**H_2-), 28.2 (Br-C(**C**H_3)-), 28.3 (-COO-CH_2**C**H_2CH_2-), 29.4 (-$CH_2(CH_2)_{15}$**C**H_2-), 29.4 (-**C**$H_2(CH_2)_{15}CH_2$-), 29.8 (-CH_2(**C**H_2)$_{15}CH_2$-), 32.0 (-**C**$H_2CH_2CH_3$), 44.7 (Br-**C**-), 59.1 (**C**H_3O-), 61.7 (Br-C(CH_3)-CH_2-), 65.1(-COO-**C**$H_2CH_2CH_2$-), 70.5 (-O-**C**H_2**C**H_2O-), 175.8 (-**C**OO-$(CH_2)_{21}CH_3$), 176.8 (-**C**OO-CH_2CH_2-). **(P6) FTIR (cm^{-1}):** 2916 C-H stretch, 2848 C-H stretch, 1728 C=O stretch, 1467 C-H bend, 1244 C-C stretch, 1145 C-O stretch, 719 C-H rock.

Synthesis of Poly(ethylene oxide)-*block*-(Poly(octadecyl methacrylate)-*co*-Poly(docosyl methacrylate)

The method for the synthesis of PEO-*b*-(PODMA-*co*-PDSMA) was as follows; Cu(I)Br (33 mg, 0.23 mmoles) was placed in a 50 mL Schlenk tube with a magnetic stirrer. The PEO macroinitiator (1.00g, 0.45 mmoles) was dissolved in xylene:IPA mixture (9:1) (4 mL) and then added to the Schlenk tube along with PMDETA (79 mg, 0.45 mmoles) and DSMA (dissolved in xylene:IPA) (1.61 g, 4.08 mmoles). ODMA (1.38 g, 4.08 mmoles) was run through an alumina column to remove the stabiliser and then added to the Schlenk tube. The Schlenk tube was sealed and the mixture was degassed (N_2) for 1 hour. The mixture was then stirred at 95°C for 24 hours under nitrogen. After 24 hours the reaction was stopped by exposure to air and diluting with THF. The mixture was run through an alumina column to remove the catalyst and ligand and the solvent was evaporated off (rotary evaporator). The polymer was precipitated out into methanol drop wise at 0°C. The block copolymer was characterised using ^{1}H-NMR, ^{13}C-NMR, FT-IR and GPC. This method was used to produce the following % ratios of PODMA:PDSMA : 50:50, 25:75, 75:25 and 40:60.

(P2) ^{1}H NMR (400 MHz, $CDCl_3$, ppm) δ: 0.88 (triplet, 3H, -$(CH_2)_{21}$-C**H_3**, -$(CH_2)_{17}$-C**H_3**), 1.02 (broad peak, 3H, -CH_2-C-C**H_3**), 1.28 (broad peak, 38H, -(C**H_2**)$_{19}$-, -(C**H_2**)$_{15}$-), 1.60 (broad peak, 2H, -C**H_2**-$(CH_2)_{19}$-), 3.38 (singlet, 3H, C**H_3**O-), 3.65 (broad triplet, 4H, -O-C**H_2CH_2**-O-), 3.92 (broad peak, 2H, -COO-C**H_2**-). **(P2) ^{13}C NMR ($CDCl_3$, ppm) δ:** 14.2 (-CH_2CH_2**C**H_3), 18.5 (-C(**C**H_3)$_2$-) 22.7 (-CH_2**C**H_2CH_3), 26.2 (-COO-CH_2CH_2**C**H_2-), 28.2 (Br-C(**C**H_3)-), 28.3 (-COO-CH_2**C**H_2CH_2-), 29.5 (-$CH_2(CH_2)_{15}$**C**H_2-), 29.5 (-$CH_2(CH_2)_{11}$**C**H_2-), 29.5 (-**C**$H_2(CH_2)_{15}CH_2$-), 29.5 (-**C**$H_2(CH_2)_{11}CH_2$-), 29.8 (-CH_2(**C**H_2)$_{15}CH_2$-), 29.8 (-CH_2(**C**H_2)$_{11}CH_2$-), 32.0 (-**C**$H_2(CH_2)CH_3$), 54.4 (Br-**C**-), 59.1 (Br-C(CH_3)-**C**H_2-), 61.6 (**C**H_3O-), 65.0 (-COO-**C**$H_2CH_2CH_2$-), 70.5 (-O-**C**H_2**C**H_2O-), 177.6 (-**C**OO-$(CH_2)_{21}CH_3$), 176.7 (-**C**OO-CH_2CH_2-). **(P2) FTIR (cm^{-1}):** 2916 C-H stretch, 2848 C-H stretch, 1728 C=O stretch, 1465 C-H bend, 1242 C-C stretch, 1145 C-O stretch, 719 C-H rock.

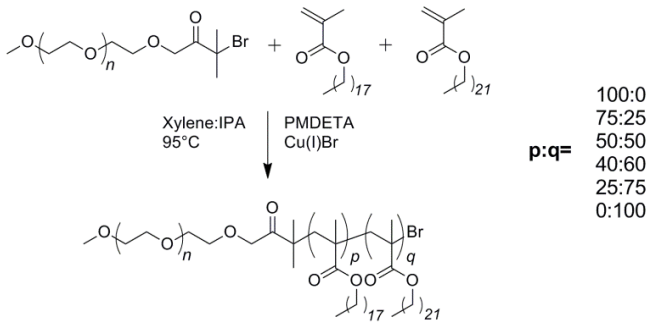

Scheme 1: Synthesis of block copolymer poly(ethylene oxide)-block-(poly(octadecyl methacrylate)-random-poly(docosyl methacrylate)) via ATRP using a PEO macroinitiator.

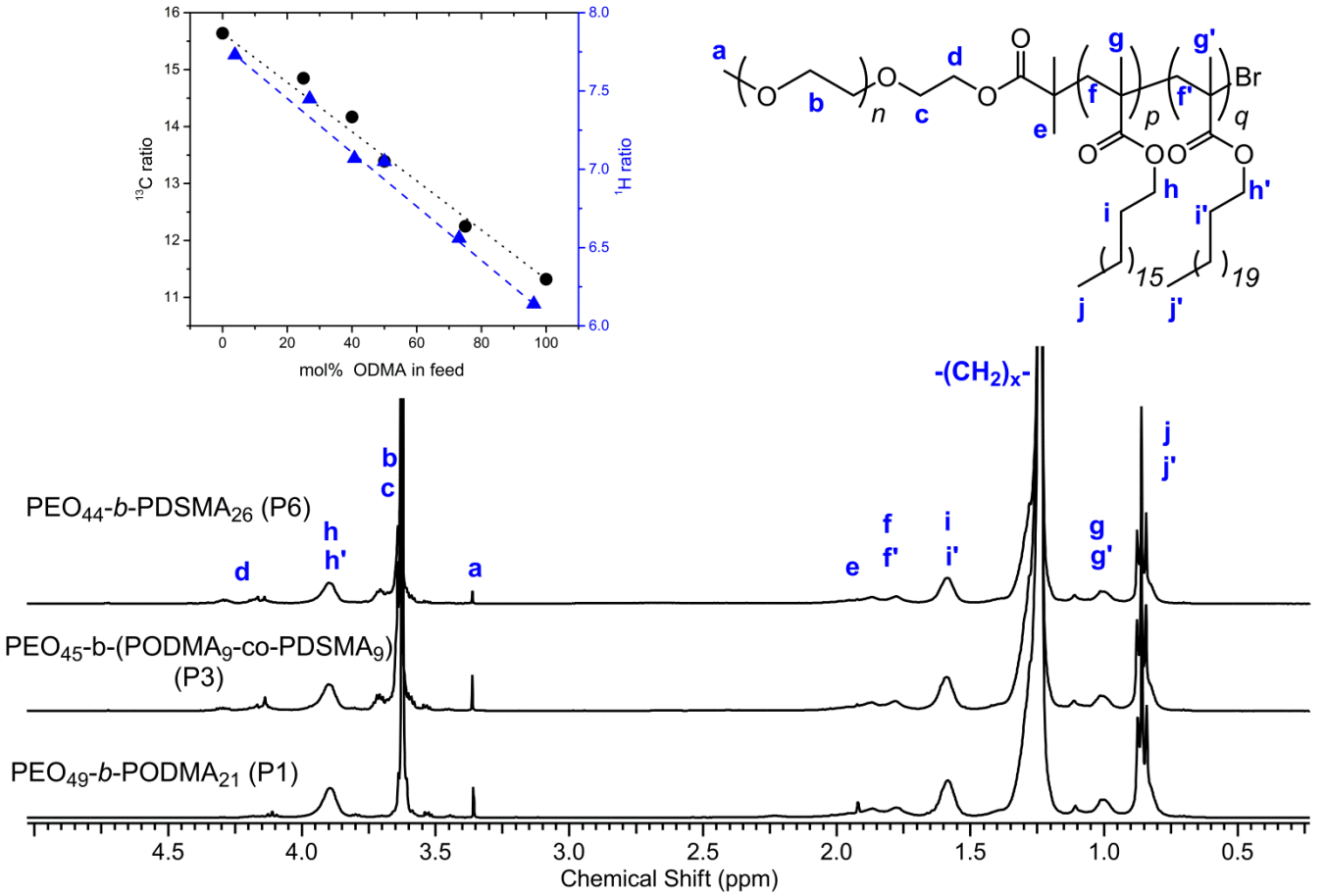

Figure 1: NMR spectra of poly(ethylene oxide)-*block*-(poly(octadecyl methacrylate)-*random*-poly(docosyl methacrylate)) via ATRP using a PEO macroinitiator. The graphical inset shows the plot of ODMA feed versus the ratio of CH_2 to CH_3 intergrals from ^{13}C and ^{1}H NMR for the synthesied copolymers (see text for further detail).

Results and Discussion

Synthesis and Characterisation

A modification of a well reported literature method[6-8, 27] was used for the synthesis of the PEO_{49}-*b*-$PODMA_{21}$ homopolymer via ATRP using a PEO macroinitiator and a Cu(I)Br/PMDETA catalyst (Scheme 1). The same procedure was also followed for the synthesis of the PEO-*b*-PDSMA homopolymer and the PEO-*b*-(PODMA-*co*-PDSMA) copolymers. In all cases the wt% of PEO within the block copolymer was maintained at 25 wt% and all reactions went to greater than 97% conversion according to NMR spectroscopic analysis of the reaction mixtures. Molecular weight parameters were determined relative to PMMA standards in THF by SEC. The final PEO:poly(alkyl methacrylate) compositions of the copolymers were determined from ^{1}H NMR spectroscopy (Figure 1a). Whereas the high conversion of the copolymerisations (97%+) indicated that the feed ratio should match the final composition of ODMA:DSMA in the copolymers, this could not be directly determined from ^{1}H or ^{13}C NMR with any degree of accuracy given that the chemical differences between the monomers were minimal. Similar difficulties in determining the ratio of alkyl acrylate monomers in copolymers was previously reported by O'Leary and Paul.[22] However by modifying a method described in their report we measured the ratio of the integrals in both ^{13}C and ^{1}H NMR spectra of the central CH_2 peaks (at 29.0 to 31.2 ppm and 1.15 to 1.45 ppm respectively) and the CH_3 terminal peaks (at 14.2 ppm and 0.85 ppm respectively). Provided the ratio of octadecyl to docosyl monomers in the copolymer chain matches that of the feed ratio the plots of these ratios should be linear. As shown in Figure 1 (inset) plots with linear fits with R^2 values of 0.99 were obtained for both ^{1}H and ^{13}C ratios indicating that the

Table 1: Molecular weight parameters for block copolymers.

ID	Structure	M_n[a]	M_w/M_n[a]	M_n[b]	ODMA:DSMA[c]
P1	PEO_{49}-*b*-$PODMA_{21}$	15400	1.29	9499	100:0
P2	PEO_{45}-*b*-($PODMA_{15}$-*co*-$PDSMA_4$)	11100	1.13	8850	75:25
P3	PEO_{45}-*b*-($PODMA_9$-*co*-$PDSMA_9$)	11100	1.12	8792	50:50
P4	PEO_{45}-*b*-($PODMA_7$-*co*-$PDSMA_{11}$)	12100	1.13	8915	40:60
P5	PEO_{45}-*b*-($PODMA_5$-*co*-$PDSMA_{13}$)	10800	1.12	9016	25:75
P6	PEO_{44}-*b*-$PDSMA_{16}$	10500	1.20	8475	0:100

a. Measured by SEC.
b. Measured by ^{1}H NMR. c. Feed ratio ODMA:DSMA

copolymer chain composition matches that of the feed ratio. The degree of polymerization of each block copolymer was close to that predicted and the dispersities were all below 1.3 indicating narrow size distributions (Table 1). The M_n values observed from both ^{1}H-NMR and GPC are significantly different. This was expected for a comb-like block copolymer such as PEO-*b*-PODMA and has been observed previously for polymers with a comb-like block such as PEOGMA and poly(octadecyl acrylate). The difference is due to the hydrodynamic volume of the BCP being significantly different to that of the linear PMMA standards (used to calibrate the GPC) at the same molecular weight.[28, 29] The GPC measurements do however provide a good indication to the dispersities of the polymer chain.

Thermal Analysis of the Bulk BCPs

The phase transitions of the block copolymers were determined by analysis with differential scanning calorimetry. Introducing DSMA as a portion or all of the hydrophobic block should allow manipulation of the T_m, as the longer the alkyl side chain the greater the degree of crystallinity and the higher the melting point. The expected temperature range for the homo and copolymers was between 21 and 40°C, i.e. between the melting range of PODMA and PDSMA homopolymers. Values for D_c and T_m are given in given in Table 2. Figure 2a shows the DSC thermograms for all the bulk block copolymers. P1 (PEO_{49}-*b*-$PODMA_{21}$) exhibited a melting transition (T_m) of 21.3°C which was attributed to the melting of the semi-crystalline PODMA block (ODMA T_m: 18-20°C). This result is consistent with previous observations for the same BCP.[6-8, 22]

The change in enthalpy of fusion (ΔH_f) values given in Table 2 were calculated from the peak area (J/g) using Equation 1. Where A is the area (J/g), MW is the average molecular weight of the side-chain repeat unit ((MW C18 x mol%) + (MW C22 x mol%)) and the result was multiplied by 1.25 to take into account the fact that the hydrophobic block represents only 75% of the BCP.

$$\Delta H_f = A\left(\frac{1}{1000}\right)\text{MW x } 1.25 \qquad \text{Equation 1}$$

Overall as the wt% of PDSMA was increased the T_m increased. This means an increase in average side chain length increases the T_m as observed previously in the literature.[15, 21] This clearly demonstrates that modification of the semi-crystalline hydrophobic block, allows the thermal properties of the bulk BCPS to be easily tailored.

Table 2: DSC melting transition values for PEO-b-PODMA, PEO-b-PDSMA and all PEO-b-(PODMA-co-PDSMA) copolymers. All values are taken from the second heating run.

ID	Average side-chain length[a]	Peak (˚C)	T_m onset (˚C)	ΔH_f (kJ/mol)[b]	D_c (%)	ODMA: DSMA mol ratio
P1	18	26.6	21.5	9.78	16.0	100:0
P2	18.8	32.4	23.6	8.64	13.5	75:25
P3	20	36.2	29.7	12.55	18.5	50:50
P4	20.44	39.5	31.1	19.53	28.1	40:60
P5	20.88	42.5	31.9	23.48	33.1	25:75
P6	22	46.0	41.3	18.64	24.9	0:100

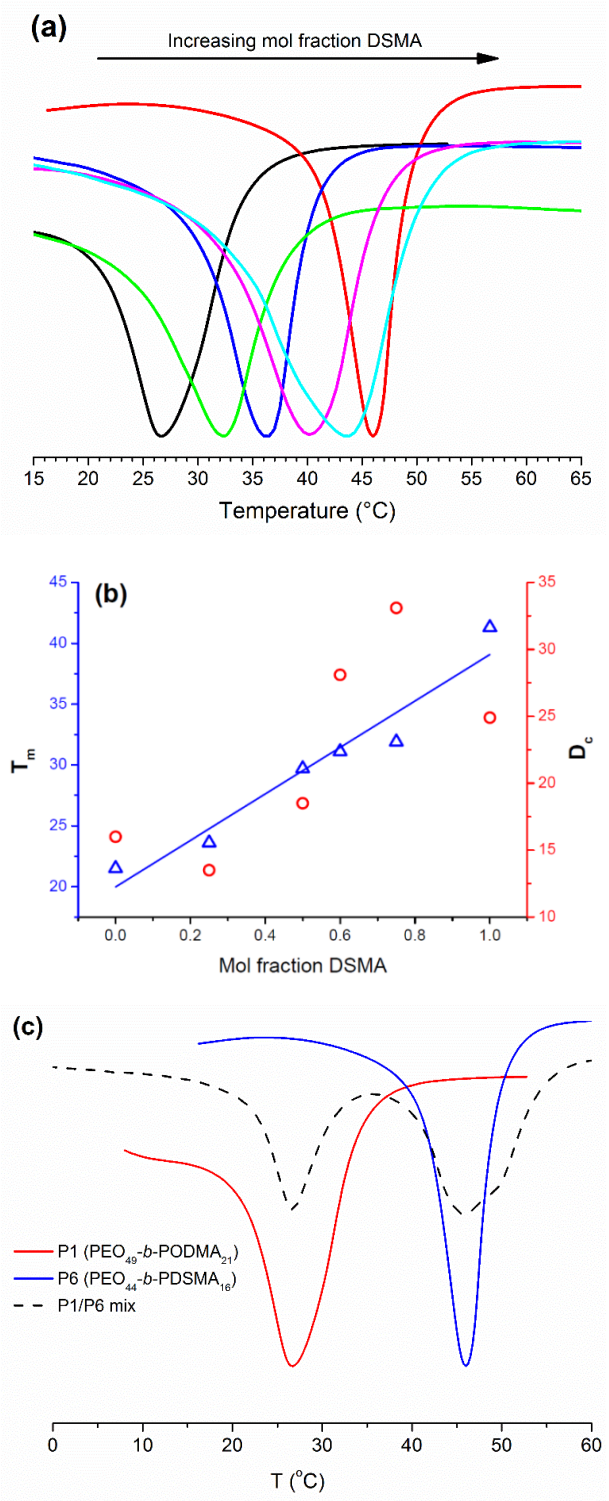

Figure 2: (a) DSC thermograms (2nd heating run) of PEO-b-(PODMA-co-PDSMA) copolymers; ODMA: DSMA mol ratio, black 100:0 (P1) , green 75:25 (P2), blue 50:50 (P3), magenta 40:60 (P4), cyan 25:75 (P5), red 0:100 (P6). (b) DSMA mol fraction v degree of crystallinity, Dc melting transition(Tm). (c) DSC thermogram of a 50:50 (wt%) blend of bulk P1 (PEO44-b-PODMA19) and P6 (PEO44-b-PDSMA16) both with a PEO wt% of 25%.

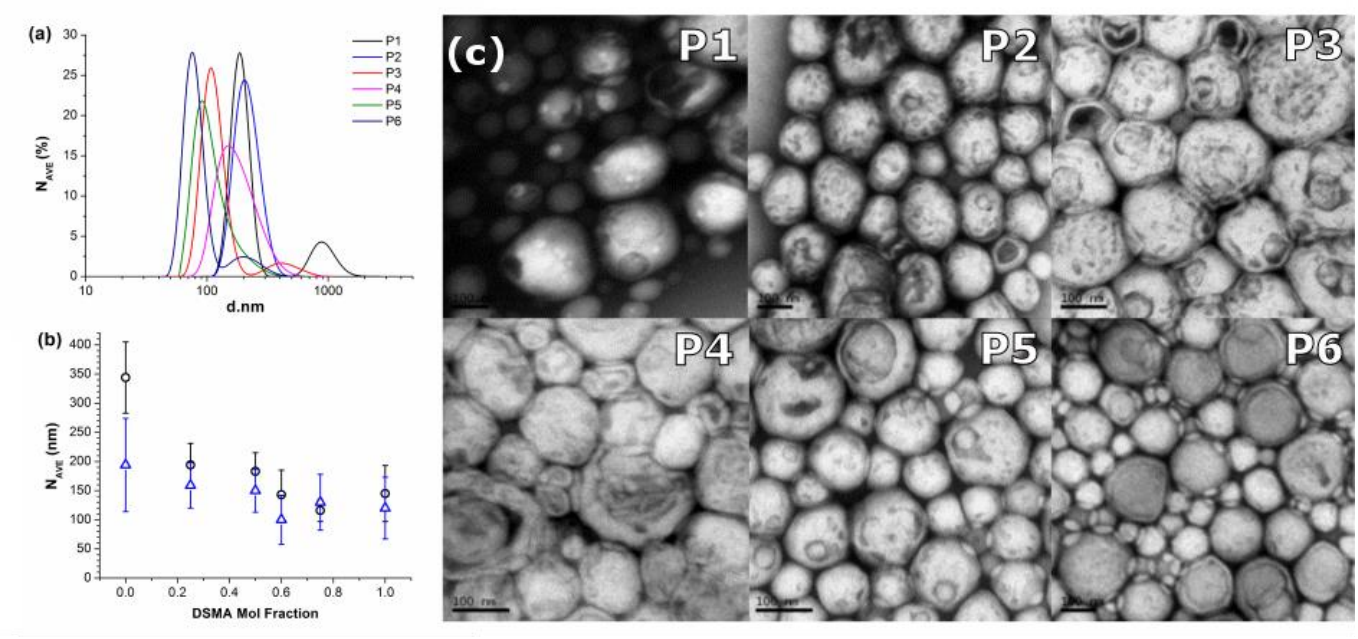

Figure 3: (a) DLS number average distribution plots for P1-P6 (5 wt %) aggregate dispersions. (b) Plot of N_{ave} (black circles from DLS, blue triangles from TEM) of P1 (PEO_{49}-*b*-$PODMA_{21}$), P2-P5 (PEO-*b*-(PODMA-*co*-PDSMA) and P6 (PEO_{44}-*b*-$PDSMA_{12}$) particles (5 wt%) against the DSMA mol fraction. (c) TEM images of P1 4 wt% (0 wt % DSMA), P2 5 wt%, P3 5 wt%, P4 5 wt%, P5 5 wt% and P6 5 wt% aggregates; negatively stained with 5% uranyl acetate and 1% acetic acid. All scale bars represent 100 nm.

The degree of crystallisation (D_C) of the alkyl side chains was then calculated from the ΔH_f using Equation 2 where ΔH_f is the enthalpy change of fusion for the hydrophobic block and $q_{m,CH2}$ is the heat of melting per CH_2 unit in the alkyl side chain, this was calculated to be 3.4 kJ/mol as established by Beiner *et al.* from DSC measurements of octadecane.[30]

$$D_c = \frac{\Delta H_f}{q_{m,CH_2}} x\ 10 \qquad \text{Equation 2}$$

The D_c calculated for P1 was 16%, Beiner *et al.* reported a D_c value of 31% for a homopolymer of PODMA with a similar chain length (DP-27).[31] A possible reason for this decrease in D_c may be due to the contribution of PEO to inhibiting self-organisation of the PODMA backbone, which in turn hinders the side chains ability to achieve crystalline order.[15, 23, 31-33] A PEO-*b*-PODMA BCP has previously been demonstrated to adopt a bicontinuous microphase separated structure in which case crystallisation will be further hampered by the cylinder-like morphology (in contrast to lamellar).[15, 22] Figure 2b illustrates the effect of increasing PDMSA wt% upon the D_c. Initially there is a slight decrease in D_c from 0% DMSA to 25% DSMA which was expected as the octadecyl side chains will pack together to form a crystalline order more easily than a mixture of side chain lengths. The decrease in D_c seen from 75% DSMA to 100% DMSA could be due to the decrease in DP of the hydrophobic block from 19 for the copolymers to 16.

A 50:50 wt% blend of P1 and P6 (Figure 2c) showed two distinct melting transitions by DSC, resulting from the melting of the octadecyl side chains in P1 and the melting of the docosyl side chains in P6. This indicates that the copolymerisation of these two monomers is necessary to achieve the co-crystallisation of the alkyl side chains. This was expected based on the observations of Paul *et al.* who found that the length of the alkyl chains needs to be similar for co-crystallisation to occur. [34] They observed that a 50:50 blend of poly(octadecyl acrylate) and poly(docosyl acrylate) prepared by solution casting films gave an inhomogeneous blend.

Self-Assembly of Bicontinuous Nanospheres

In principle the simplest approach to manipulating the melting temperature of any PEO-*b*-alkyl methacrylate copolymer aggregate would be to self-assemble and thereby co-crystallise two or more copolymers with distinct melting temperatures. However as discussed in the previous section the PEO-*b*-PODMA and PEO-*b*-PDSMA copolymers do not co-crystallise and phase separation was evident. To confirm that copolymers would not co-crystallise in aggregate structures a 50:50 wt% mix of P1 (200 mg) and P6 (200 mg) was dissolved in THF (4 ml). Water (6 ml) was then slowly added to this solution and the THF was removed via dialysis against 3 L of water at 35°C over 24 hours. However this resulted in the formation of white precipitate that settled to the bottom of the dialysis cassette and no stable dispersion.

Aggregate dispersions of the BCPs P1-P6 were prepared by the same dialysis method, first by the dissolution of the BCP (0.5 g) in THF (4 mL (P1)/6 mL (P2-P6)) at 35°C for P1 and 45°C for P2-P6 followed by the slow addition of water (6mL for P1 and 4 mL for P2 to P6). The THF was removed via dialysis against 3 L of water at 35°C or 45°C over 24 hours. The aggregate dispersions were prepared at 4 wt% (P1) and 5 wt% (P2-P6) in 10 mL of water.[6] The aggregate solutions were analysed with dynamic light scattering (Figure 3a and 3b) and TEM (Figure 3c). The distributions showed either, bimodal distributions

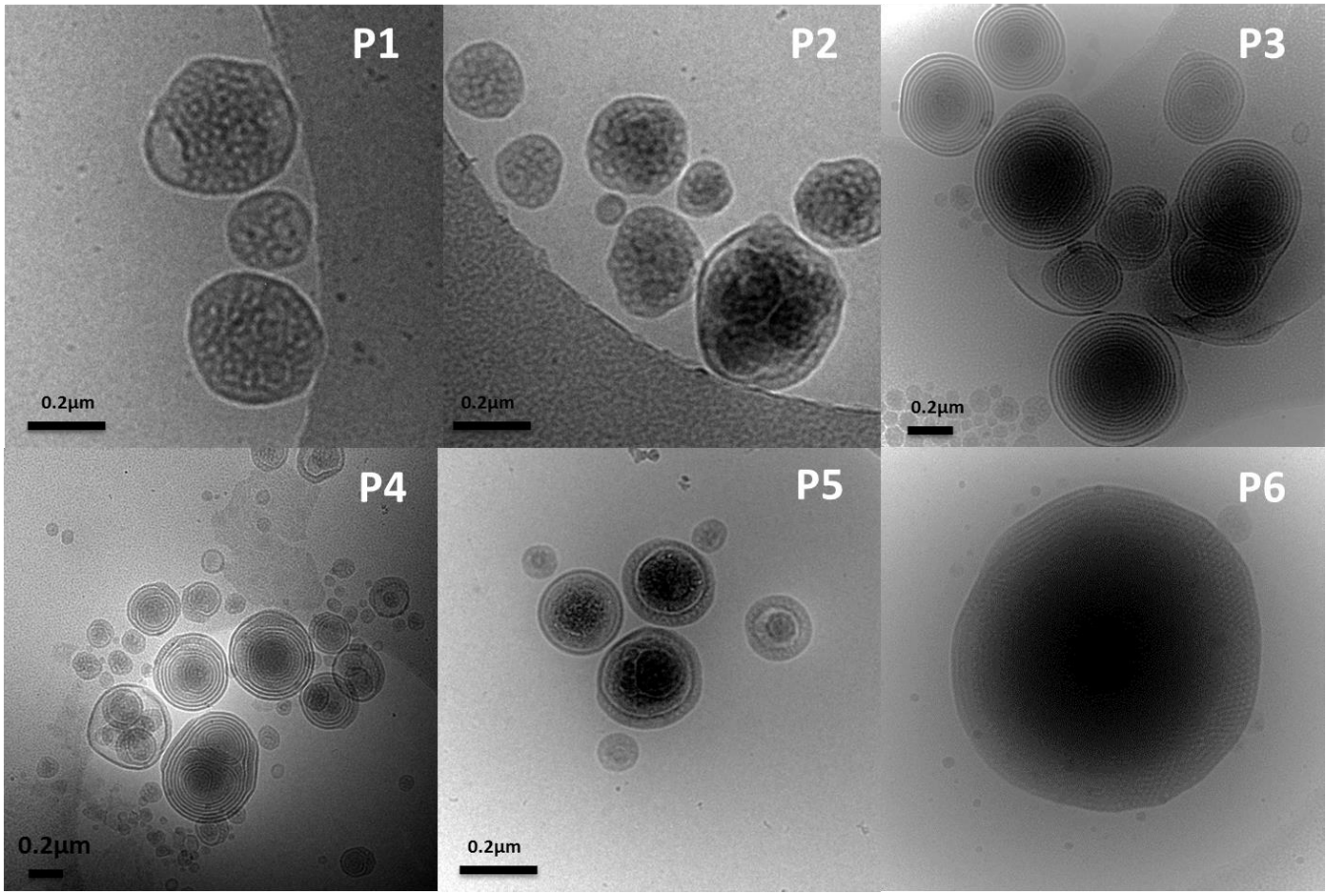

Figure 4: Cryo-TEM images of aqueous dispersions of bicontinuous nanospheres P1 4 wt%, P2 5 wt%, P3 5 wt%) P4 5 wt%, P5 5 wt% and P6 5 wt%.

with a significant distribution of smaller particles (d ≈ 70 to 120 nm) and a smaller distribution of larger diameters particles (d ≈ 150 to 1000 nm), or monomodal distributions with low diameter maxima and a tail to higher diameters. However neither a bimodal distribution of particles nor particles with diameters >300 nm were evident in the TEM micrographs suggesting that the higher diameter particles measured by DLS were transient aggregates formed from association of the smaller particles. Overall the aggregate sizes recorded by TEM (Figure 3b and 3c) were similar to those recorded by DLS with the exception of P1 (PEO_{49}-*b*-$PODMA_{21}$) in which case the N_{ave} diameter was significantly larger than that of the TEM values. There is no immediate explanation for this discrepancy. Generally the average particle diameter showed a slight decrease with increasing mol fraction of DSMA in the copolymer structures though the significance of this is open to interpretation. The TEM micrographs in all cases suggest some degree of internal structure for the aggregates and in particular P2 and P3 appear to show bicontinuous morphologies.

To study the internal morphology of the aggregates upon introduction of the DSMA monomer into the copolymer structures the aggregate solutions were analysed using cryo-TEM (Figure 4 and Figures S16 to S20).

It has already been well established that PEO-*b*-PODMA self-assembles into BPNs at 0.1, 0.5 and 4 wt% in solution when the weight fraction, *f*, of PEO in the copolymer is between 15-25%.[7]. As expected PEO-*b*-PODMA (P1) showed exclusively a BPN morphology as did P2. Copolymer P3 (ODMA:DSMA = 50:50) appeared to form predominantly multi-lamellar structures with some bicontinuous spheres whilst P4 and P5 formed spheres with complex cores (possibly bicontinuous) and multi-lamellar coronae (from a single lamella layer to many) as well as simple bicontinuous spheres, with the former tending to be larger in diameter than the latter. In contrast P6 appeared to form just bicontinuous spheres once more. Since cryo-TEM does not readily allow for the imaging of as many aggregates as TEM the relative sizes and distributions of morphologies is merely qualitative. No immediate conclusions can therefore be drawn about the effect of copolymerisation in the hydrophobic block beyond the general observations that no unexpected morphologies are observed and bicontinuous and mult-lamellar predominate. The phase diagram (molecular weight versus hydrophilic block fraction) for PEO-*b*-PODMA copolymer aggregates has demonstrated that there is considerable overlap between the lamellar and bicontinuous morphology regions and this agrees with the observations here.[7]

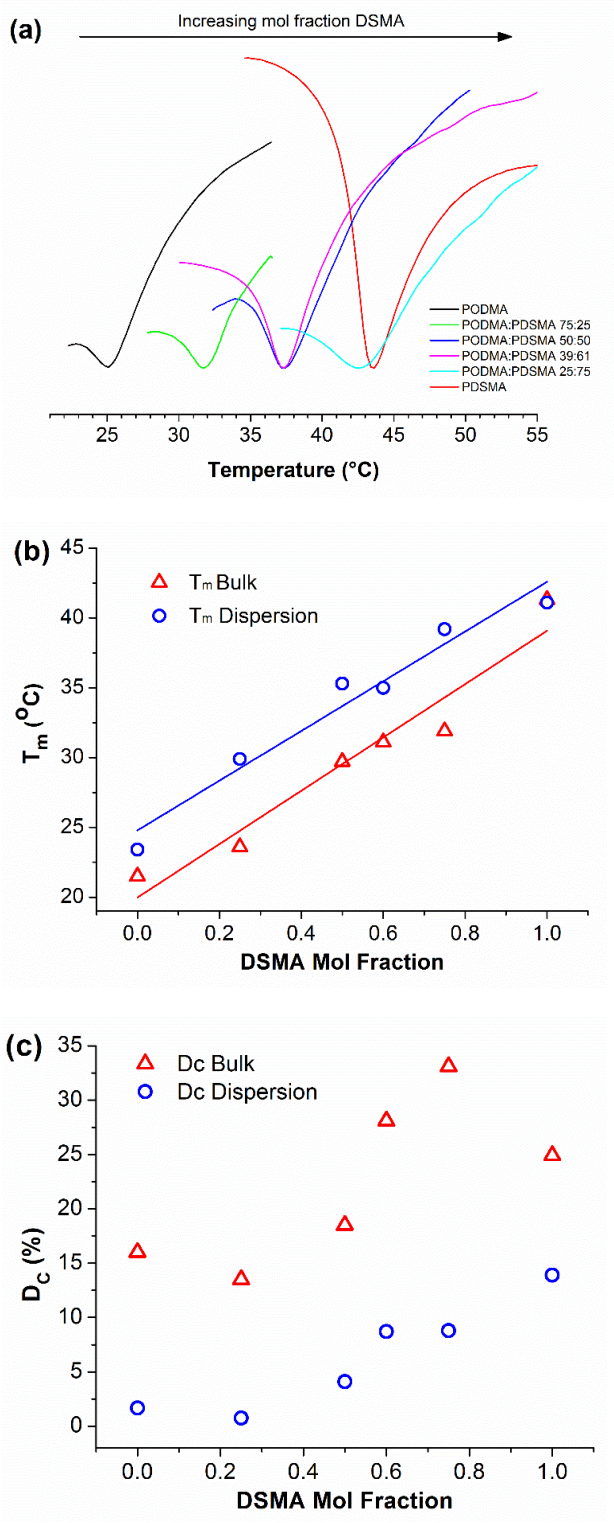

Figure 5: (a) DSC thermograms of PEO-*b*-(PODMA-*co*-PDSMA) aggregates (P1 to P6) at 5 wt% in solution, with increasing mol fraction of DSMA. ODMA: DSMA ratio, black 100:0, green 75:25, blue 50:50, magenta 40:60, cyan 25:75, red 0:100. (b) Onset melting transitions (measured by DSC) of both bulk and dispersion (5 wt %) samples against DSMA mol fraction; lines are linear fits to two sets of data. (c) Degree of crystallisation (calculated from DSC) of both bulk and dispersion (5 wt %) samples against DSMA mol fraction

DSC Analysis of Bicontinuous Nanospheres

DSC measurements of the aggregate dispersions were carried out against a reference pan containing an equivalent volume of water (relative to sample pan). The normalised DSC thermograms of the aggregate solutions are shown in Figure 5a. Whilst there is some overlap of peak melting temperatures at higher DSMA content, the onset melting temperatures displayed the same trend as observed for the bulk samples, where an increase in DSMA wt% results in an increase in T_m (Figure 5b). The T_m values for the aggregate dispersions however were on average 4.1 ± 2.9 °C higher than those for the bulk samples. This difference was particularly pronounced for the copolymers containing ODMA and DSMA, possibly a result of some degree of inhibition of ODMA crystallisation in the confined dimensions of the aggregates leading to the DSMA melting being more pronounced. This interpretation is supported by the reduced degrees of crystallinity displayed by the aggregates in comparison to the bulk samples. The ΔH_f and D_c values for all aggregate samples in dispersion are given in Table 3. ΔH_f and D_c were calculated as previously described for the bulk samples (Equation 1 and 2). However as the BCP weight only represents 4 wt% for P1 and 5 wt% for P2-P6 the measured values were multiplied by 0.25 and 0.20 to reflect the alkyl methacrylate contents respectively. The D_c values for the aggregate dispersions were significantly lower than those recorded for the bulk samples (Figure 5c). There are two possible explanations for this result: (i) that due to the constraints of the aggregate morphologies (bicontinuous and multi-lamellar spheres) the crystal packing of the side-chains was inhibited to a significant degree; (ii) incomplete or suppressed crystallisation of the ODMA side-chains. Hempel et al. have previously reported D_c values for bulk PODMA samples (varying chain lengths) of 29 ± 1.4(SD) % and further reported Dc values for polystyrene-*block*-poly(octadecyl methacrylate) of a similar magnitude for both cylindrical and lamellar microphase separated morphologies. This suggests that confining alkyl methacrylate side chains to small segregated regions need not inhibit crystallisation. This is not surprising since it has been observed that long alkyl chains on poly (meth)acrylate backbones aggregate into nano-domains in the melt (nanophase separation) and the subsequent crystallisation of the side-chains occurs between adjacent polymer backbones that are ~3-4 nm apart.[30, 31, 35] There is no immediate means of demonstrating any incomplete

Table 3: DSC melting transition values for PEO-b-PODMA, PEO-b-PDSMA and all PEO-b-(PODMA-*co*-PDSMA) copolymer aggregates solutions at 5 wt% in solution. All values are taken from the second heating run.

ID	Average side-chain length[a]	Peak (˚C)	T_m onset (˚C)	ΔH_F (kJ/mol) [b]	D_c (%)[c]	ODMA: DSMA mol ratio
P1	18	24.9	23.4	1.03	1.7	100:0
P2	18.8	31.8	29.9	0.48	0.75	75:25
P3	20	37.3	35.3	2.78	4.1	50:50
P4	20.44	37.3	35.0	6.05	8.7	40:60
P5	20.88	42.4	39.2	6.24	8.8	25:75

P6	22	43.5	41.1	10.36	13.9	0:100

crystallisation of the octadecyl side-chains, however O'Leary and Paul have previously demonstrated no inhibition of crystallinity for a series of crystalline alkyl acrylate copolymers; i.e. different alkyl chains can co-crystallise. The low concentrations of polymer in the aggregate solutions gave small thermal transitions in comparison to the bulk samples, making exact measurements of the transition enthalpies difficult (see SI) and consequently the Dc values must be assumed to have a relatively low degree of accuracy. The use of microcalorimetric measurements will allow for more accurate measurements of the heat flow and therefore the D_c in future studies. Furthermore, given the importance of thermal history to degrees of crystallinity in semi-crystalline polymers some degree of annealing is likely to increase this in the aggregates. However the results still demonstrate the control achieved over the T_m, simply by manipulating the average alkyl side chain length within the hydrophobic block.

Encapsulation and controlled release of Ibuprofen

Three polymers were chosen to make polymer aggregate dispersions with encapsulated ibuprofen; the block copolymers P1 and P6 containing homo ODMA and DSMA blocks respectively and P5 with the ODMA:DSMA molar ratio of 25:75. P1 and P6 give T_m (onset) values at each end of the melting range scale and P5 has a melting temperature just above typical human body temperatures (Table 3). The conditions followed for self-assembly were similar to those employed for the preparation of the aggregate dispersions of P1 to P6 but employing a solution of ibuprofen in THF in place of pure THF. 1 wt% aggregate dispersions of the BCPs P1, P5 and P6 were prepared by the dissolution of the BCP (0.1 g) and ibuprofen (0.02 g) in THF (6 mL) followed by the slow addition of water. Both P5 and P6 ibuprofen containing dispersions gave aggregates (P5-IB and P6-IB) with size distributions similar to those prepared in the absence of ibuprofen with N_{ave} = 408 and 354 nm for P5-IB and P5 respectively and N_{ave} = 420 and 431 nm for P6-IB and P6 respectively (Figure 6, ESI). In contrast P1-IB formed aggregates with average diameters of 60 nm (N_{ave}) compared to the average of 530 nm recorded for P1. It is thought that the ibuprofen was changing the hydrophilic-hydrophobic balance in the BCP aggregates. This was not surprising as ibuprofen has been seen to aggregate in solution by itself and interacts with polymers during self-assembly in order to solubilise in water.[36, 37] A different dispersion was therefore formed using P7 a PEO-*b*-PODMA sample with 15 wt% PEO. After dialysis the resulting P7-IB dispersion was observed to form aggregates with number-average diameters of 226 nm and this sample, along with P5-IB and P6-IB, was used in the subsequent release studies.

CryoTEM studies of P7-IB showed that the aggregates were bicontinuous (Figure 6d) and the TEM studies of the P8-IB aggregates showed that they were predominantly spherical and where internal morphology could be seen were multi-lamellar with some bicontinuous spheres (Figure 6c). The

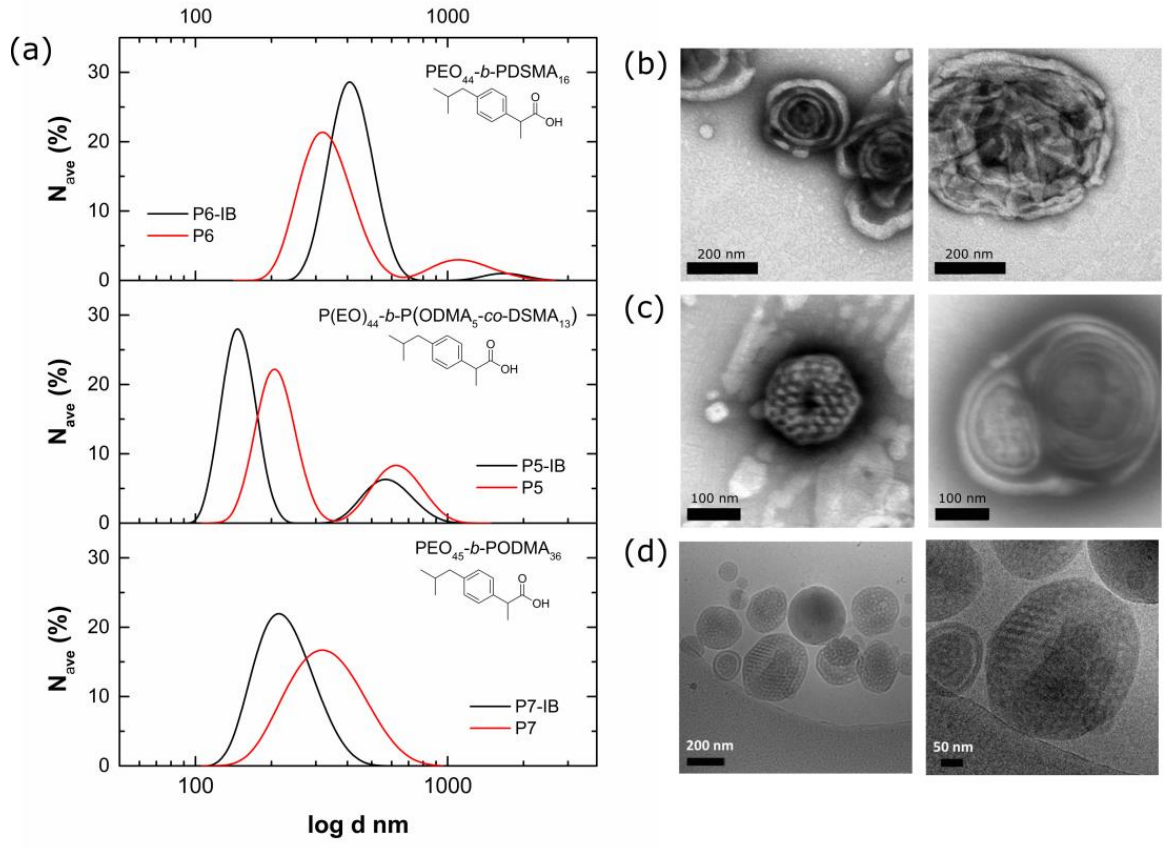

Figure 6: (a) DLS number average particle size distribution plots for P7-IB, P5-IB and P6-IB dispersions in water. TEM micrographs of aqueous dispersions of (b) P5-IB, (c) P6-IB and cryo-TEM micrographs of aqueous dispersions of (d) P7-IB.

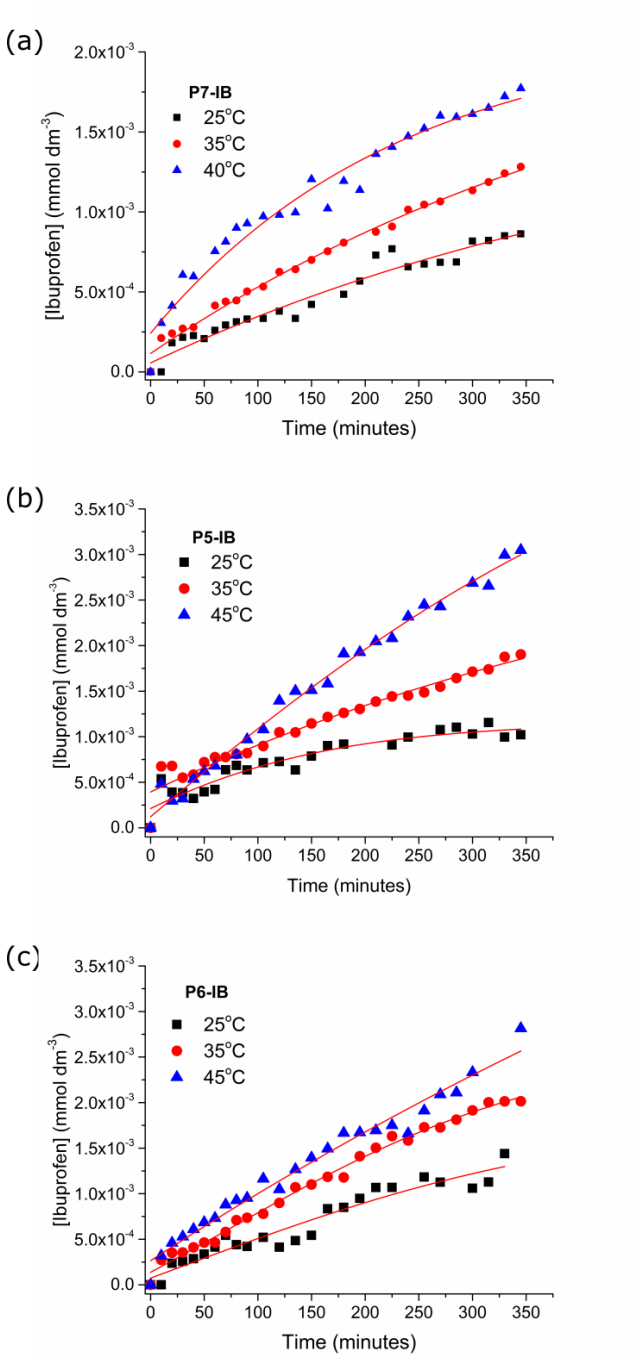

Figure 7: Ibuprofen release profiles at different temperatures for (a) P7-IB, (b) P5-IB and (c) P6-IB dispersions in water.

morphology of the aggregates as observed by TEM in the P9-IB dispersions were complex and could best be described as spheres consisting of concentric thick lamella and/or folded (crumpled) layers (Figure 6b). Again it is apparent that more detailed cryoTEM studies are required to fully ascertain the effect that ibuprofen inclusion has on the internal morphologies. Samples of P7-Ib, P5-IB and P6-IB dispersions (1 cm^3) were placed in a Quixsep dialyser sealed with a dialysis membrane and gently stirred in an excess of water (0.75 dm^3) over 6 hours at various temperatures (25, 35, 40 and 45 °C). Samples were taken at intervals over this period and subject to HPLC analysis to determine ibuprofen concentrations. The resulting release profiles for the three samples at different temperatures are shown in Figure 7. The absolute amount of ibuprofen encapsulated in the aggregates could not be directly determined by UV-vis spectroscopy due to considerable overlap between the absorption due to carbonyls of the polymer and that of the phenyl ring of the ibuprofen (ESI). Thus to estimate total amount encapsulated after preparation the release data for the dispersions for each sample at each temperature were fitted with a sigmoidal curve and extrapolated until a constant value was reached. This enabled the plotting of release profiles based on fractional release (Figures 8a and 8b). The profiles show a decrease in relative release rates with DSMA content in the hydrophobic block; after 350 minutes for the PEO-*b*-PODMA (P7) ~80% of ibuprofen has been released and for the PEO-*b*-PDSMA (P6) ~30% has been released. Furthermore all samples showed an increase in release rate with an increase in temperature.

Values for the release rates were taken from the linear fit of the release profiles at release fractions from 0.1 to 0.4 onwards (Figure 8b). These values are given in Table 4 and plotted in Figure 9a. Figure 9b compares the change in release relative to the rate at 25 °C. The onset melting temperatures of the aggregate without ibuprofen in dispersion are also shown in both plots. It is apparent from these plots that the fastest release rates correspond to P7-IB which at 25 °C is expected to be partially or completely melted and at 35 and 40 °C will be completely melted. Consequently P5-IB with no crystalline content and fluid interiors shows the highest release rates. In stark contrast P6-IB which at 25 and 35 °C is semi-crystalline shows much smaller release rates and surprisingly the rate remains small at 45 °C suggesting that melting has not occurred despite the expected transition starting at ~41 °C. It is possible that the presence of the ibuprofen raises melting temperatures but more likely the use of onset temperatures is misleading and the peak values of T_m (Table 3) would be more appropriate. Future work will address this issue. The general increase in release rates with temperature for both P7-IB and P6-IB can be attributed to increased diffusion coefficients which should follow an Arrhenius relationship.[38]

The P5-IB sample in contrast to both P7-IB and P6-IB shows intermediate values with clear evidence of significant increases in the release rate upon going from 25 °C to 45 °C. With an onset melting transition of 39.2 °C the hydrophobic semi-crystalline core undergoes a transition to a wholly amorphous

Table 4. Release rates at each temperature for copolymer-ibuprofen dispersions.

		Release rate (s^{-1} x 10^5)		
Sample	ODMA:DSMA	25 °C	35 °C	40/45 °C
P7-IB	100:0	1.7	2.4	2.7
P5-IB	25:75	0.54	1.3	2.4
P6-IB	0:100	0.59	0.89	1.1

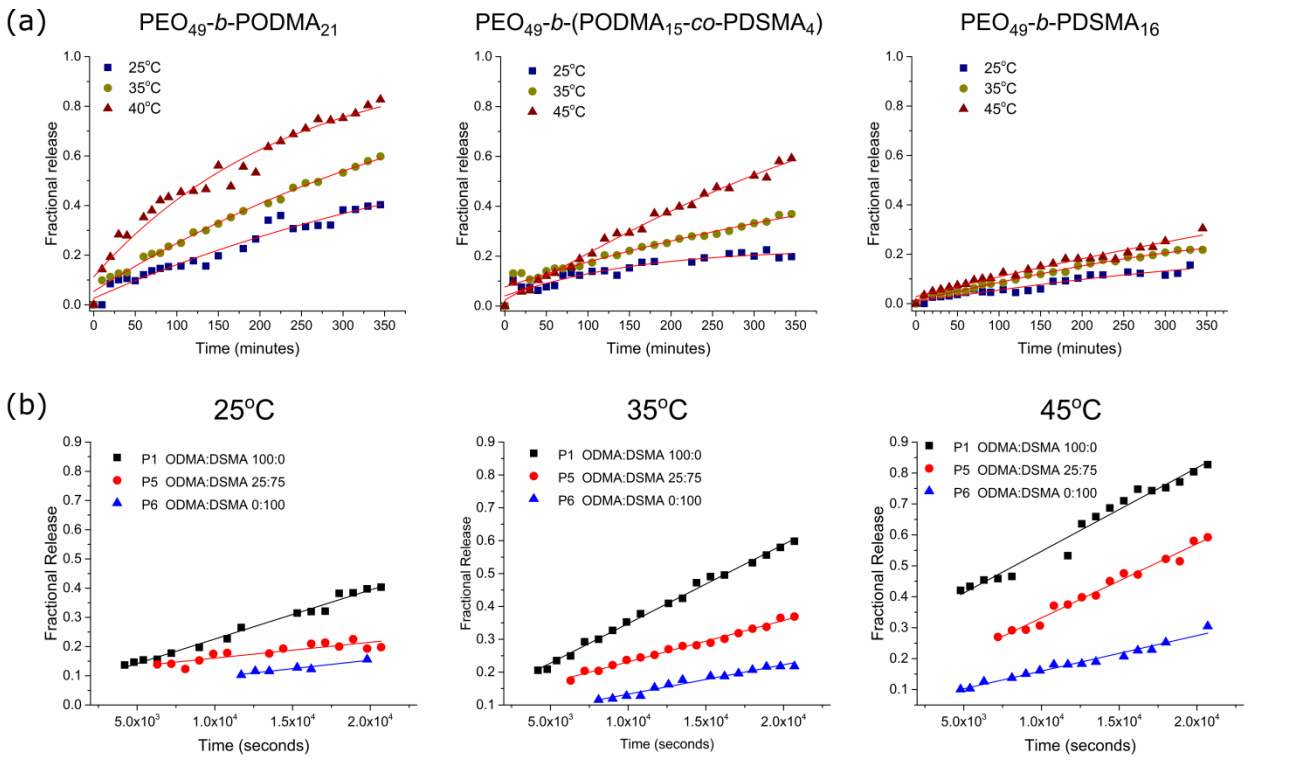

Figure 8: Fractional release profiles for ibuprofen release from (a) each copolymer dispersion and (b) for each temperature.

state and increased polymer mobility significantly enhancing release rates of the ibuprofen. This is wholly in agreement with the previously reported study of the rate of release of pyrene from a PEO-*b*-PODMA block copolymer aggregate. The role of both crystallinity and temperature in the controlled release from semi-crystalline aggregates is illustrated by the plot of release rates versus temperature and degree of crystallinity shown in Figure 9c. It is apparent that the degree of

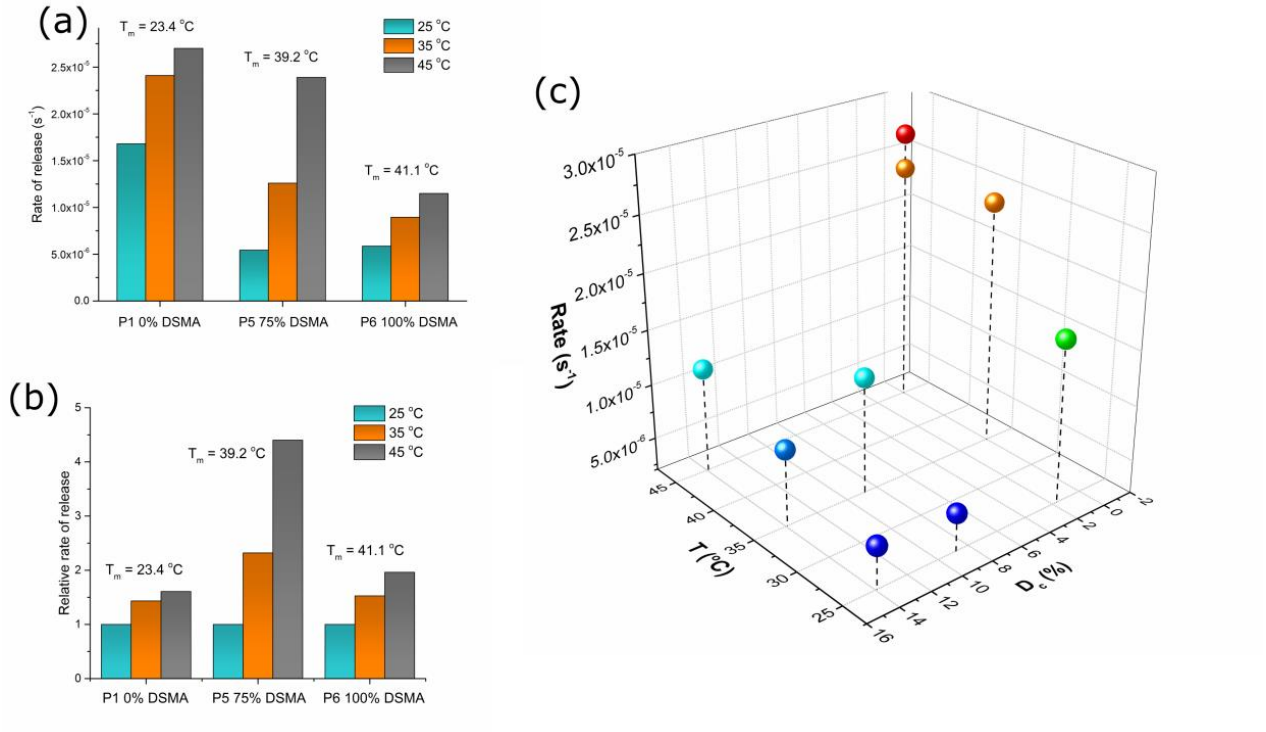

Figure 9: (a) Absolute rate constant for all samples. (b) Rate constants relative to that at25 C. (c) Variation in rate constant versus onset melting temperature (T_m) of aggregate dispersions and degree of crystallinity (D_c).

crystallinity in the aggregates is a strong determinant of the release behaviour of the ibuprofen. Whilst this is unsurprising in that multiple studies have demonstrated the correlation between increased permeability of molecules through semi-crystalline (co)polymers with lower degrees of crystallinity this effect has not hitherto been observed for semi-crystalline aggregates.[20, 23, 38-41]

Conclusion

A range of semi-crystalline amphiphilic block copolymers have been synthesised with a PEO hydrophilic block and varying ratios of ODMA to DSMA monomer (from 0:100 to 100:0) in the hydrophobic block. In the bulk state these block copolymers displayed a steadily increasing melting point from 21.5 to 41.3 °C with increasing fraction of DSMA to ODMA. When self-assembled in aqueous colloidal dispersions the spherical aggregates adopted predominantly bicontinuous and multi-lamellar internal morphologies. These aggregates displayed melting transitions that closely matched those of the bulk state samples across the range 23.4 to 41.1 °C. This work demonstrates the possibility of manipulating the thermal response of the hydrophobic interior component of self-assembled block copolymers in aqueous dispersions, either as a complementary or alternative property to the commonly employed hydrophilic component thermal response. Preliminary experiments on measuring the rate of release of ibuprofen from the block copolymer aggregates in aqueous dispersions were undertaken. These demonstrated that the degree of crystallinity of the hydrophobic alkyl methacrylate block correlated with release rate, where higher degrees of crystallinity led to lower rates. Consequently when heated above the melting temperature of the hydrophobic block the release rate for one of the aggregate dispersions was observed to dramatically increase. This demonstrated the application of a hydrophobic block based temperature switch to control release rates from block copolymer aggregates.

Acknowledgements

We wish to acknowledge University of Kent for a PhD studentship in support of this work.

References

1. S. J. Holder and N. A. J. M. Sommerdijk, *Polymer Chemistry*, 2011, **2**, 1018-1028.
2. C. Cheng, H. Wei, B.-X. Shi, H. Cheng, C. Li, Z.-W. Gu, S.-X. Cheng, X.-Z. Zhang and R.-X. Zhuo, *Biomaterials*, 2008, **29**, 497-505.
3. P. Schattling, F. D. Jochum and P. Theato, *Polymer Chemistry*, 2014, **5**, 25-36.
4. C. Sanson, O. Diou, J. Thévenot, E. Ibarboure, A. Soum, A. Brûlet, S. Miraux, E. Thiaudière, S. Tan, A. Brisson, V. Dupuis, O. Sandre and S. Lecommandoux, *ACS Nano*, 2011, **5**, 1122-1140.
5. C. Sanson, J. F. Le Meins, C. Schatz, A. Soum and S. Lecommandoux, *Soft Matter*, 2010, **6**, 1722-1730.
6. B. E. McKenzie, F. Nudelman, P. H. H. Bomans, S. J. Holder and N. A. J. M. Sommerdijk, *Journal of the American Chemical Society*, 2010, **132**, 10256-10259.
7. B. E. McKenzie, H. Friedrich, M. J. M. Wirix, J. F. de Visser, O. R. Monaghan, P. H. H. Bomans, F. Nudelman, S. J. Holder and N. A. J. M. Sommerdijk, *Angewandte Chemie International Edition*, 2015, **54**, 2457-2461.
8. S. J. Holder, G. Woodward, B. McKenzie and N. A. J. M. Sommerdijk, *RSC Advances*, 2014, **4**, 26354-26358.
9. B. E. McKenzie, J. F. de Visser, G. Portale, D. Hermida-Merino, H. Friedrich, P. H. H. Bomans, W. Bras, O. R. Monaghan, S. J. Holder and N. A. J. M. Sommerdijk, *Soft Matter*, 2016, **12**, 4113-4122.
10. J. W. Nichols and Y. H. Bae, *Journal of Controlled Release*, 2014, **190**, 451-464.
11. H. Kobayashi, R. Watanabe and P. L. Choyke, *Theranostics*, 2014, **4**, 81-89.
12. H. Maeda, *Journal of Controlled Release*, 2012, **164**, 138-144.
13. C. Rehberg and C. Fisher, *Industrial & Engineering Chemistry*, 1948, **40**, 1429-1433.
14. H. Kaufman, A. Sacher, T. Alfrey and I. Fankuchen, *Journal of the American Chemical Society*, 1948, **70**, 3147-3147.
15. S. A. Greenberg and T. Alfrey, *Journal of the American Chemical Society*, 1954, **76**, 6280-6285.
16. E. F. Jordan, D. W. Feldeisen and A. Wrigley, *Journal of Polymer Science Part A-1: Polymer Chemistry*, 1971, **9**, 1835-1851.
17. E. F. Jordan, B. Artymyshyn, A. Speca and A. Wrigley, *Journal of Polymer Science Part A-1: Polymer Chemistry*, 1971, **9**, 3349-3365.
18. S. Prasad, Z. Jiang, S. K. Sinha and A. Dhinojwala, *Physical review letters*, 2008, **101**, 065505.
19. H. Hsieh, B. Post and H. Morawetz, *Journal of Polymer Science: Polymer Physics Edition*, 1976, **14**, 1241-1255.
20. K. A. O'Leary and D. R. Paul, *Polymer*, 2006, **47**, 1226-1244.
21. K. A. O'Leary and D. R. Paul, *Polymer*, 2006, **47**, 1245-1258.
22. K. O'Leary and D. Paul, *Polymer*, 2004, **45**, 6575-6585.
23. Z. Mogri and D. R. Paul, *Polymer*, 2001, **42**, 7765-7780.
24. M. Frouws, E. Bastiaannet, R. Langley, W. Chia, M. van Herk-Sukel, V. Lemmens, H. Putter, H. Hartgrink, B. Bonsing and C. Van de Velde, *British Journal of Cancer*, 2017.
25. Y. Liu, J.-Q. Chen, L. Xie, J. Wang, T. Li, Y. He, Y. Gao, X. Qin and S. Li, *BMC medicine*, 2014, **12**, 55.
26. F. M. Shebl, A. W. Hsing, Y. Park, A. R. Hollenbeck, L. W. Chu, T. E. Meyer and J. Koshiol, *PloS one*, 2014, **9**, e114633.
27. B. E. Mkenzie, S. J. Holder and N. A. J. M. Sommerdijk, *Current Opinion in Colloid & Interface Science*, 2012, **17**, 343-349.
28. A. Rudin and H. L. W. Hoegy, *Journal of Polymer Science Part A-1: Polymer Chemistry*, 1972, **10**, 217-235.
29. M. Gaborieau and P. Castignolles, *Analytical and Bioanalytical Chemistry*, 2011, **399**, 1413-1423.
30. E. Hempel, H. Budde, S. Höring and M. Beiner, *Thermochimica Acta*, 2005, **432**, 254-261.

31. E. Hempel, H. Budde, S. Höring and M. Beiner, *Journal of Non-Crystalline Solids*, 2006, **352**, 5013-5020.
32. K. Yokota, T. Kougo and T. Hirabayashi, *Polym J*, 1983, **15**, 891-898.
33. T. Hirabayashi, T. Kikuta, K. Kasabou and K. Yokota, *Polym J*, 1988, **20**, 693-698.
34. B. S. Kirkland and D. R. Paul, *Polymer*, 2008, **49**, 507-524.
35. M. Beiner and H. Huth, *Nature materials*, 2003, **2**, 595-599.
36. M. A. Rub, N. Azum, D. Kumar, A. M. Asiri and H. M. Marwani, *The Journal of Chemical Thermodynamics*, 2014, **74**, 91-102.
37. A. Ridell, H. Evertsson, S. Nilsson and L.-O. Sundelöf, *Journal of Pharmaceutical Sciences*, 1999, **88**, 1175-1181.
38. S. C. George and S. Thomas, *Progress in Polymer Science*, 2001, **26**, 985-1017.
39. K. O'Leary and D. Paul, *Polymer*, 2006, **47**, 1245-1258.
40. Z. Mogri and D. Paul, *Polymer*, 2001, **42**, 7765-7780.
41. Z. Mogri and D. Paul, *Journal of Polymer Science Part B: Polymer Physics*, 2001, **39**, 979-984.